

## Physical Origin of Dynamic Ion Transport Features through Single Conical Nanopores at Different Bias Frequencies

Dengchao Wang, Juan Liu, Maksim Kvetny, Yan Li, Warren Brown, and Gangli Wang\*.

Department of Chemistry, Georgia State University, Atlanta, GA, 30302, [glwang@gsu.edu](mailto:glwang@gsu.edu)

**Scheme SI-1** Schemes of the gradient SCD on the glass surface.

**Table SI-1** Boundary conditions for this numerical solution based on Poisson and Nernst-Planck equations.

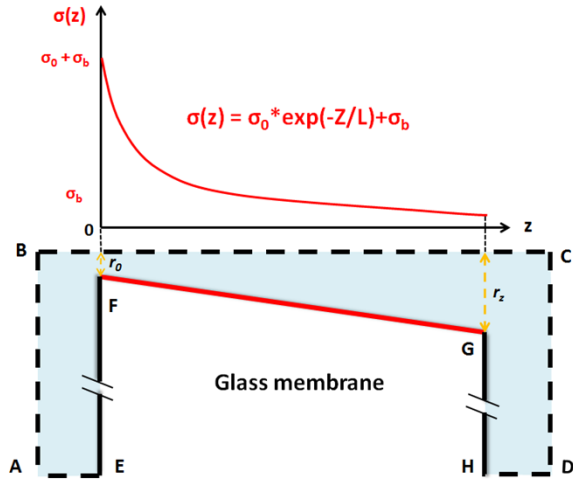
**Fig.SI-1** Experimental  $I$ - $V$  frequency features from an 80 nm radius nanopore in 1 mM KCl at different scan rates.

**Fig.SI-2** Subtraction of capacitive charging current from the experimental  $I$ - $V$  responses shown in Fig.1.

**Fig.SI-3** The simulated current from Models with different membrane radius (EF) and channel length (BC).

**Fig.SI-4** The fitting of the experiments with gradient and uniform SCD.

**Fig.SI-5** The fitting of the experimental results for a 60 nm radius nanopore in 10 mM KCl.



**Scheme SI-1.** Definition of the gradient surface charge density (SCD) on the interior glass surface at the transport-limiting nanopore region.

### Finite elements simulation details

Because the nanopore geometry has center line symmetry, a symmetrical 2D modal was built to lower the simulation demand. The flux and current were obtained via the surface integration at the electrode (AB or CD).

In the nanopore membrane model shown in Scheme SI-1, the depth of conical shape nanochannel is 10  $\mu\text{m}$  and the half-cone angle is set as  $11^\circ$ . Two reservoirs with a dimension of  $30 \times 2 \mu\text{m}$  are connected to the nanochannels. Therefore, EF and GH represent the exterior surfaces of the glass membrane. If the extra surfaces (size of GH) are removed in the two reservoirs, the conical nanochannel structure is represented by the Model 1 in Scheme 2 in the main text. The gradient surface charge density (SCD) is introduced to address the overestimated low conductivity state current when a uniform SCD is applied. The boundary conditions used to solve the Poisson and Nernst-Planck equations are summarized in Table SI-1. Free triangular mesh elements were used. For the applied potential waveform, the sampling rate (or potential step size) is 12 mV. Two full cycles were applied in each simulation. The results from the second scan were presented and analyzed.

**Table SI-1.** Boundary conditions defined in the numerical solution of Nernst-Planck and Poisson equation. The boundaries are illustrated in Scheme SI-1.

Boundary	Physical properties	Boundary condition
BC	Axial symmetry, Z axis	
AB	Working electrode	Applied potential, $V=f(t)$
AE&HD	insulator	Zero charge
EF&GH	Glass membrane surface	Constant SCD = $-1 \text{ mC/m}^2$
FG	Glass wall	Gradient SCD (Exponential decay)
CD	Reference electrode, ground	$V = 0$

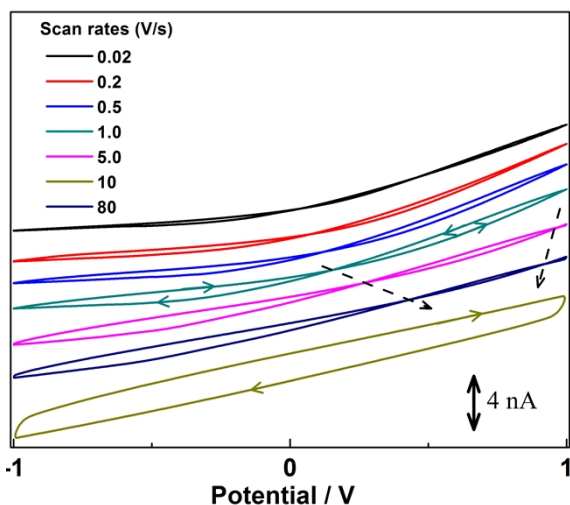


**Fig.SI-1** Experimental  $I$ - $V$  frequency features from an 80 nm radius nanopore in 1 mM KCl at different bias frequencies. Similar behaviors can be observed from this nanopore under different scan rates: at relatively slow scan rate (0.02 V/s), rectification of steady-state current is observed and at medium scan rates (0.2 to 1.0 V/s), pinched hysteresis loops emerge and superimpose with the rectified current curves. When the scan rate goes higher (5 to 10 V/s), capacitive charging/discharging current is superimposed over the nanopore transport current, and finally dominate the current responses at very high scan rate (80 V/s).

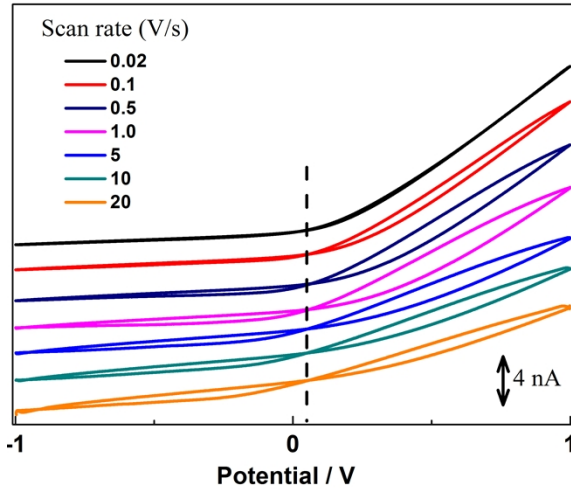


**Fig.SI-2** Subtraction of capacitive charging current from the experimental  $I$ - $V$  responses shown in Fig.1.

The experimental total current signals from the 200 nm nanopore in 1 mM KCl were processed. At low scan rates when the cross point potential remains constant, a 58 mV effective transmembrane potential is obtained. The gap currents at this non-shifting potential at higher scan rates were then used to compute the charging current curve over the full potential range. The pure transport-through current was obtained by subtracting the capacitive charging/discharging current loops from that measured experimentally. The processed experimental  $I$ - $V$  curves agree well with the simulation results using the model 1 without the large membrane.

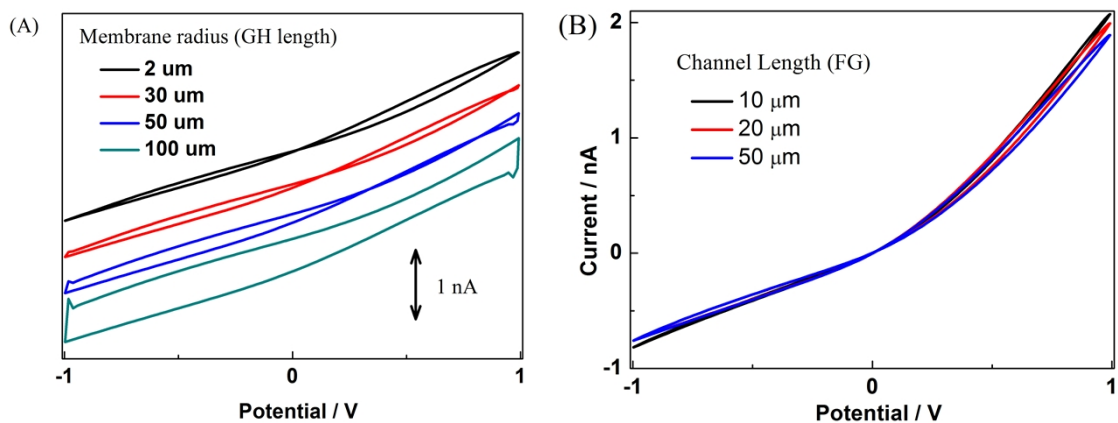


**Fig.SI-3** Simulated current using model 2 at (A) different membrane radius (GH) and (B) different channel length (FG). A constant SCD of  $-0.01 \text{ C/m}^2$  is applied on FG. The KCl concentration is 1 mM with the scan rate at 1000 V/s in the simulation.

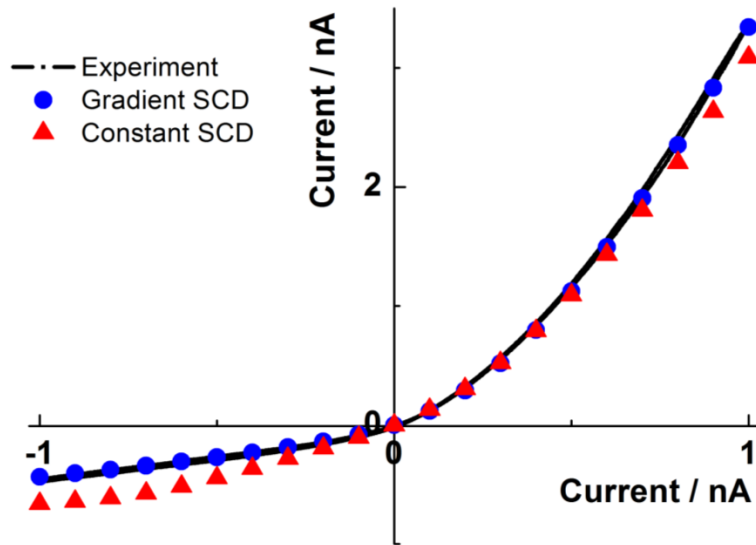


**Fig.SI-4** Fitting of experimental results by using gradient and uniform SCD definitions. The experimental  $I$ - $V$  response was collected from the 60 nm radius nanopore in 1 mM KCl.

First, by systematic variation of the SCD value uniformly defined on FG, a constant value of  $-0.03 \text{ C/m}^2$  would give a good fitting shown as the red triangles. Note further increase could match the high conductivity state current better, but make the low conductivity side worse (overestimating the current). By the variation of the distribution length  $L$  ( $L=1.6 \mu\text{m}$ ) in a gradient SCD definition using the maximum value of  $-0.03 \text{ C/m}^2$  founded above, excellent fitting at both high and low conductivity states are shown as blue dots.

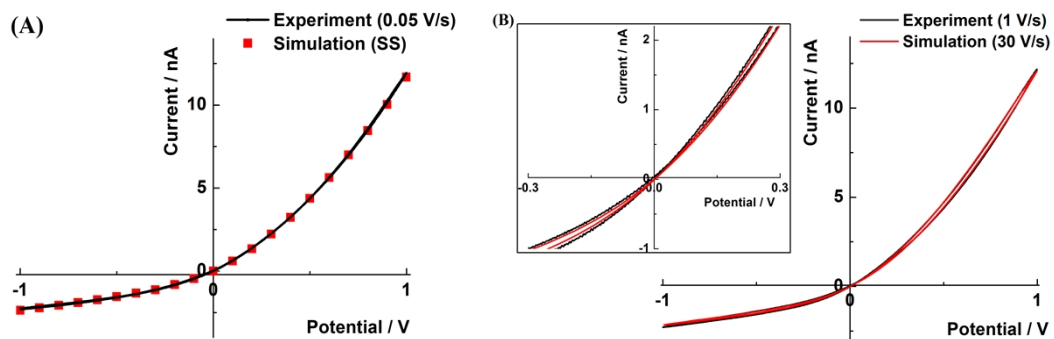


**Fig.SI-5** Fitting of the experimental results from a 60 nm radius nanopore in 10 mM KCl at different scan rates. (A) The correlation of the low scan rate experiments (0.05 V/s) with steady state simulation. (B) The correlation of medium scan rate experiments (1 V/s) with time-dependent simulation (30 V/s). The fitting parameters are  $\sigma_0 + \sigma_b = -0.045 \text{ C/m}^2$ , and the distribution length  $L$  is  $0.6 \text{ }\mu\text{m}$ .